



Endogenous S-nitrosocysteine proteomic inventories identify a core of proteins in heart metabolic pathways

Benjamin Lau^{a,b}, Hossein Fazelinia^{c,d}, Ipsita Mohanty^b, Serena Raimo^b, Margarita Tenopoulou^e, Paschalis-Thomas Doulias^e, Harry Ischiropoulos^{b,*}

^a Swarthmore College, Swarthmore, PA, USA

^b Children's Hospital of Philadelphia Research Institute and Departments of Pediatrics, The Raymond and Ruth Perelman School of Medicine at the University of Pennsylvania, PA, 19104, USA

^c Proteomics Core Facility, Children's Hospital of Philadelphia, Philadelphia, PA, USA

^d Department of Biomedical Health and Informatics, Children's Hospital of Philadelphia, Philadelphia, PA, USA

^e Laboratory of Biochemistry, Department of Chemistry, School of Sciences, University of Ioannina, Greece

ARTICLE INFO

Keywords:

Nitric oxide
S-nitrosylation
Proteomics
Cardiovascular system

ABSTRACT

Protein cysteine residues are essential for protein folding, participate in enzymatic catalysis, and coordinate the binding of metal ions to proteins. Enzymatically catalyzed and redox-dependent post-translational modifications of cysteine residues are also critical for signal transduction and regulation of protein function and localization. S-nitrosylation, the addition of a nitric oxide equivalent to a cysteine residue, is a redox-dependent modification. In this study, we curated and analyzed four different studies that employed various chemoselective platforms coupled to mass spectrometry to precisely identify S-nitrosocysteine residues in mouse heart proteins. Collectively 1974 S-nitrosocysteine residues in 761 proteins were identified and 33.4% were identified in two or more studies. A core of 75 S-nitrosocysteine residues in 44 proteins were identified in all four studies. Bioinformatic analysis of each study indicated a significant enrichment of mitochondrial proteins participating in metabolism. Regulatory proteins in glycolysis, TCA cycle, oxidative phosphorylation and ATP production, long chain fatty acid β -oxidation, and ketone and amino acid metabolism constitute the major functional pathways impacted by protein S-nitrosylation. In the cardiovascular system, nitric oxide signaling regulates vasodilation and cardiac muscle contractility. The meta-analysis of the proteomic data supports the hypothesis that nitric oxide signaling via protein S-nitrosylation is also a regulator of cardiomyocyte metabolism that coordinates fuel utilization to maximize ATP production. As such, protein cysteine S-nitrosylation represents a third functional dimension of nitric oxide signaling in the cardiovascular system to ensure optimal cardiac function.

1. Introduction

The enzymatic generation of nitric oxide (NO) by nitric oxide synthases (NOS) provides spatial and temporal signaling that accomplish diverse paracrine and autocrine biological functions. Canonical NO signaling involves the binding of NO to the penta-coordinated heme center of the β subunit of soluble guanylate cyclase (sGC) [1–4]. The activation of sGC triggers the conversion of guanosine triphosphate to cyclic guanosine monophosphate (cGMP). Downstream of cGMP are networks of cGMP-dependent protein kinases (PKG), primarily the Ser/Thr kinases PKG1 and PKG2. The binding of cGMP to allosteric sites in the regulatory domain of the PKG1 isozymes increases their catalytic

activity and promotes phosphorylation of several client proteins [5–8]. PKG1 α is the predominant isoform in endothelial cells, smooth muscle cells, and cardiomyocytes. This canonical signaling cascade is terminated at nearly every step through de-phosphorylation by phosphatases, removal of cGMP by phosphodiesterases, elimination of NO by competing reactions with metalloenzymes and superoxide, or termination of NO production by NOS [1–8].

Alternatively, or possibly complementary, S-nitrosation of protein cysteine residues forms S-nitrosocysteine in a cGMP-independent manner [9–12]. This post-translational modification (often designated as cysteine S-nitrosylation) is derived by a direct reaction of a NO equivalent or by S-trans-nitrosation. Our group and others have

* Corresponding author.

E-mail address: ischirop@penmedicine.upenn.edu (H. Ischiropoulos).

<https://doi.org/10.1016/j.redox.2021.102153>

Received 31 August 2021; Received in revised form 24 September 2021; Accepted 27 September 2021

Available online 1 October 2021

2213-2317/© 2021 Published by Elsevier B.V. This is an open access article under the CC BY-NC-ND license (<http://creativecommons.org/licenses/by-nc-nd/4.0/>).

proposed and documented several mechanisms for the direct formation of protein S-nitrosocysteine [13–20]. S-trans-nitrosation refers to either protein-protein or protein-small molecule S-nitrosothiol (i.e. S-nitroso-glutathione) interactions that align a nitrosothiol with a reduced protein thiol for the transfer of the NO equivalent [13–19]. Protein-protein cysteine-dependent de-nitrosylation is primarily responsible for the termination of this signal [20].

With the use of different chemoselective approaches coupled to mass spectrometry, several studies have precisely identified S-nitrosocysteine residues in proteins *in vivo* under physiological conditions and in disease [21–34]. The proteomic-based identification of S-nitrosylated proteins has enabled in-depth studies exploring the mechanisms of protein S-nitrosocysteine formation, the parameters that govern the selectivity of this modification, and the functional consequences on specific proteins or pathways. In this study, we focused on proteomic data that identified endogenous protein S-nitrosocysteine residues in naïve untreated mouse hearts. We identified four different studies performed independently in four laboratories using different chemoselective platforms [22–25]. All these studies reported the proteins and sites of cysteine S-nitrosation offering a unique opportunity for data meta-analysis. The meta-analysis included (i) manual curation of the data sets for each study, (ii) generation of a combined S-nitrosocysteine proteome, (iii) identification of a core of proteins and cysteine residues common in all four studies, (iv) a report on the biological function and cellular localization of the S-nitrosylated proteins, and (v) biophysical and structural information for the commonly shared modified cysteine residues. Factors that may contribute to the differences among the four different studies are discussed. Collectively the data support the hypothesis that protein S-nitrosylation in mouse heart fine tunes ATP production and utilization to secure optimal function.

2. Methods

2.1. Inclusion criteria and study selection

The following criteria were employed for inclusion in this analysis:

1. Studies were performed in wild type C57BL/6 mice between the ages of 2–8 months either using whole hearts or the left ventricle (experimental details are listed in Table 1). Based on studies performed in large cohorts, mice between the ages of 3–8 months are considered mature adults, a period at which biological processes and structures are fully developed and there is no active maturational growth or signs of aging. Studies employing mice older than 8 months were excluded.
2. The mice were not subjected to any intervention or treatment.
3. The studies identified and reported the peptides with the S-nitrosocysteine residues.

Based on these criteria we included four independently performed studies that were published between 2012 and 2017. A total of 39 mice were analyzed in the four studies. Table 1 provides an overview of the experimental approach for each study; study 1 [22], study 2 [23], study 3 [24] and study 4 [25].

2.2. Overview of proteomic methods utilized for the identification of protein S-nitrosocysteine

The proteomic platforms for the identification of protein S-nitrosocysteine are divided into two categories: (i) a two-step process that includes reducing the SNO bond and tagging the reduced cysteine (studies 1, 3 and 4) and (ii) a direct one step reaction that displaces NO from SNO and conjugates a ligand to the cysteine residue (study 2). All the methods require the complete alkylation (blocking) of reduced

Table 1
Experimental approaches and methods utilized in the four studies.

	Study 1 [21]	Study 2 [22]	Study 3 [23]	Study 4 [24]
Sample size	N = 21	N = 8	N = 6	N = 4
Source	Jackson Lab	Jackson Lab	Jackson Lab	Charles River
Strain	C57BL6/J	C57BL6/J	C57BL6/J	C57BL6/J
Sex	Male	Male	Group A Female and male N = 3 Group B Male N = 3	Male
Age (months)	3–3.5	4–4.5	Group A 4–5 Group B 8	2–2.5
Perfusion	Langendorff-perfused for 60 min.	Perfusion through the left ventricle.	No perfusion.	No perfusion.
Tissue procurement	Whole heart, frozen in liquid nitrogen.	Whole heart, frozen in liquid nitrogen.	Left ventricles immediately washed and homogenized on ice.	Whole heart immediately homogenized.
Homogenization buffer and conditions	300 mM sucrose 250 mM HEPES, pH 8.0, 1 mM EDTA, 0.1 mM Neocuproine, 2.5% SDS, EDTA-free protease inhibitor tablet. 1000g for 2min	250 mM HEPES pH 7.7, 1 mM DTPA, 0.1 mM Neocuproine, 1% Triton-X-100, protease inhibitors. 13,000 g for 30 min at 4 °C	300 mM sucrose, 250 mM HEPES pH 8.0, 1mM EDTA, 0.1 mM Neocuproine, 20 mM N-ethylmaleimide NEM, EDTA-free protease inhibitor tablet. 1500 g for 2min	20% TCA containing 0.5% sulfanilamide. 16000 g at 4 °C
Blocking	Cys-TMT for 2 h at 25 °C.	20 mM MMTS in 250 mM HEPES pH 7.7, 1 mM DTPA, 0.1 mM Neocuproine, 1% Triton-x-100, 2.5% SDS, for 30 min at 50 °C.	20 mM NEM, 2.5% SDS for 20 min at 50 °C.	C ₀ -ICAT in 2% SDS, 200 mM Tris-HCl, 10 mM EDTA, 100 μM DTPA, 10 μM neocuproine.
Reduction/time	20 mM Ascorbate	NA	Group A-PBS pH 7.4, 1 mM EDTA, 0.1 mM Neocuproine pH 8.0, 5 mM sodium ascorbate Group B-1 mM CuSO ₄ + 1 mM sodium ascorbate.	10 μM CuSO ₄ and 1 mM ascorbic acid.
Labeling	20 mM ascorbate plus 5 mM cysTMTy for 2 h at 25 °C.	Solid phase organic mercury 2 h at room temperature.	Group A- 0.3 mM cysTMT and iodoTMT. Group B-Parallel labeling TMP switch assay with CysTMT/iodoTMT for 2 h at 37 °C.	Cysteine reactive cleavable ICAT reagent(C ₀ -ICAT) for 2 h at 37 °C mixed at 1400 rpm.
Generation of peptides	Trypsin digestion at 37 °C overnight.	Trypsin digestion at 37 °C for 16 h.	Trypsin digestion at room temperature overnight.	Trypsin digestion at 37 °C, overnight on mixer 1400 rpm.
MS peptide analysis	LTQ Orbitrap Velos	Q Exactive Plus Hybrid Quadrupole-Orbitrap	LTQ Orbitrap Velos	Orbitrap LTQ XL

cysteine residues to reduce false positive identifications.

2.2.1. Two step labeling platforms

Several versions of the original biotin switch methodology [21] have been developed. The method includes the generation of homogenates in a buffered solution that includes a detergent, a cysteine alkylating agent such as N-ethylmaleimide (NEM), and metal chelators such as neocuproine which prevent copper-catalyzed removal of nitric oxide from S-nitrosocysteine. Studies 1 and 3 utilized a HEPES buffered sucrose containing homogenization mixture that may favor preservation and extraction of mitochondrial proteins. Study 2 used a HEPES buffered solution without sucrose but included Triton X-100 that may facilitate mitochondrial matrix protein extraction and study 4 used a trichloroacetic acid (TCA) protein extraction solution. The homogenates are then treated with cysteine alkylating agents such as iodoacetamide or methyl methane thiosulfonate which react with reduced cysteine residues to form inert mix-disulfides. This is typically referred to as the blocking step. Next, the samples are incubated with ascorbate or Cu/ascorbate which converts S-nitrosocysteine residues to a reduced cysteine but does not impact endogenous disulfides. After ascorbate or Cu/ascorbate reduction, the newly generated reduced cysteine residues are reacted with a tag such as a cysteine-reactive tandem mass tag (cysTMT) or an iodoacetyl tandem mass tag (iodoTMT). Proteins are digested into peptides and peptides are analyzed by LC-MS/MS.

2.2.2. Direct one-step platforms

A chemoselective method for direct S-nitrosocysteine conjugation utilized organomercury reagents [16,18,29]. Organic mercury selectively reacts with reduced cysteine and S-nitrosocysteine residues to form stable mercury-thiolate conjugates. After blocking reduced cysteine residues, samples are reacted with either organomercury resin or biotin-mercury conjugates which directly enriches S-nitrosylated proteins with no cross-reactivity with disulfides. The mercury-linked proteins could be released intact using reductive chemistries and analyzed either by mass spectrometry after digestion to peptides or by western blotting. Alternatively, after extensive washing, the proteins can be digested on-column followed by extensive washing to remove unbound peptides. The column-bound peptides are released after oxidation with performic acid, which oxidizes the cysteine residues to sulfonic acid and facilitates the precise identification of the S-nitrosylated peptide by mass spectrometry. Other one step platforms such as TriAryl Phosphine (SNOTRAP) and Cys-BOOST have been developed but have not yet been used to identify endogenous S-nitrosylated proteins in the mouse heart [31–34].

2.3. Data curation and analysis

The primary data were downloaded onto Excel spreadsheets and were manually curated as follows:

1. Studies 1, 2 and 3 used perfused heart tissue. Therefore, circulating proteins serum albumin, hemoglobin, haptoglobin, immunoglobulins, hemopexin, antithrombin and fibrinogen were removed from all studies. We also removed peptides from the relatively abundant heart muscle protein Titin (Ttn, A2ASS6). All studies detected from 12 to over 100 of Titin peptides, including Titin isoforms. Titin is a rather large (molecular mass 3,906,488 Da) protein that contains numerous disulfide bonds that may be reduced during processing possibly generating false positive peptides.
2. Only unique peptides were included in the final list for the meta-analysis for each study. Peptides with alternatively cleaved trypsin sites were counted only once.
3. Peptides identified from unreviewed proteins in the UniProt knowledgebase [35] were removed.
4. Gene symbol and protein names were curated using the most recent UniProt knowledgebase (release 2021_02) www.uniprot.org.
5. Studies 1 and 3 included two datasets of control non-injured mice. The two data sets were merged to one and curated to remove duplicate values. Our previous study [23] was also merged with a new unpublished data set obtained from 4-month-old male C57BL/6 mouse hearts. The final curated data sets for each Excel file (data files 1–4) are under the tab meta-analysis.
6. The protein lists include protein isoforms given that canonical proteins and their isoforms could not always be differentiated. Isoforms share the same gene symbol and protein name but have a unique UniProt number. Protein isoforms were included and counted as separate proteins if the sites (peptides) were unique to the isoform. If the peptides were the same between the major protein and the isoform, then they were counted only once, and a / symbol indicated the major protein isoform.
7. A collective mouse heart S-nitrosocysteine proteome was constructed by combining the data from all studies and removing duplicate proteins and peptides (data file 5).
8. The precise localizations (cysteine residue modified) are indicated under cysteine location and multiple peptides from the same protein separated by commas. Most of the peptide sequences included one cysteine residue which makes the localization of the modified cysteine residue unambiguous. However, tryptic digestion occasionally produced peptides with two or more cysteine residues. Except for study 3, the other studies were not able to distinguish if one or all cysteine residues in the same peptide were modified. Thus, these cysteine residues are included in the total count as one peptide without precise localization. The location of these cysteine residues is indicated by the /symbol and studies 1, 2 and 4 included 11, 50 and 106 peptides with more than one cysteine residue, respectively. Studies 1, 3 and 4 also reported occupancy, the percent of the cysteine residue modified over the total (unmodified plus modified). These data were curated and utilized to report occupancy for S-nitrosylated peptides detected in the mouse heart.
9. Mouse heart protein abundance data were uploaded from the PAXdb: Protein Abundance Database [36] and curated. The integrated data set (combined data from several published studies) included 8309 proteins identified by mass spectrometry. Of these 8309 proteins 6301 had a numerical value for relative protein levels and were used to report abundance for the proteins identified as S-nitrosylated in the mouse heart (data file 5).
10. The gene names for the unique proteins identified for each study were submitted to Gene Ontology <http://geneontology.org> [37, 38] and analyzed for functional processes or cellular component (localization) enrichment. The same analysis was performed for the combined S-nitrosocysteine proteome (data file 5). The original, curated and analyzed data for each study and the combined proteome are found in the supplementary data files 1–4.
11. Hydropathy index was calculated using the Kyte and Doolittle amino acid hydropathy scale. Protein sequences in FASTA format were submitted to ProtScale (<https://web.expasy.org/protscale/>) and processed using an algorithm that calculates an average hydropathy value for each position in the given sequence. For each position, the algorithm considers the hydropathy index of the surrounding amino acids within the given window size. . . In this analysis, the window size was set to 9. A negative value indicates a probability that a cysteine residue is hydrophilic whereas a positive value indicates a hydrophobic cysteine residue. Secondary structure analysis was performed using the human Protein data Bank (PDB) files <https://www.rcsb.org/> and the UniProt Knowledgebase. The human and mouse sequences were aligned to ascertain the position and the conservation of the cysteine residues. The information regarding the regions of the protein

forming alpha-helices and beta strands were extracted through the PDB file. Cysteine residues that were not located within a helix or a strand were assigned to coils. The calculation of pKa values was performed using the online version of PropKa, a web-based computational prediction of pKa values of ionizable groups on macromolecules (<https://www.ddl.unimi.it/vegaol/propka.htm>). For analysis, we entered the PDB identification code which is then converted to PDB 2.2 using the VEGA algorithm. The output is passed to PropKa and its output is converted to HMTL format [39].

- Statistical analysis was performed using the GraphPad Prism 9 software. Group comparisons were performed using unpaired *t*-test with Welch's correction.

3. Results

3.1. Overview of the mouse heart S-nitrosocysteine proteomes

Fig. 1A depicts the overall number of endogenously modified proteins and peptides identified in each of the four studies after data curation. The data files for each curated study includes the original data and curated proteins and peptides with the precise cysteine localization site (Supplementary data files 1–4). The distribution of the peptides with modified cysteine residues per protein for each study is depicted in Fig. 1B. The ratio of peptides to protein was 1.64, 1.85, 1.79 and 2.24 respectively. Proteins with one S-nitrosylated cysteine residue accounted for over 50% of the proteins identified in the four studies. Proteins modified in one, two, or three cysteine residues accounted for over 80% of the proteins identified in each study (Fig. 1C).

3.2. Comparison of the four proteomic studies

The Venn diagram in Fig. 2A indicates the overlap between the proteins with S-nitrosocysteine residues in the four studies without considering the site (cysteine residue) of modification. The fraction of proteins identified in each study that was unique (proteins identified only in one study), relative to the size of the proteome, varied from 2.2% in study 1 which had the fewer proteins and peptides to 27.1% in study 4 which identified the most proteins and peptides. Collectively, 42.1% of the proteins were identified in two or more studies with 80 proteins identified in all four studies. Comparison of study 2 and study 3, which are similar in size but were acquired by the two different platforms, did not reveal any differences in the distribution of proteins shared among the other studies. This observation suggests that the enrichment approach is not contributing to the discordance in protein identification.

We constructed an adult mouse heart S-nitrosocysteine proteome by assembling all the proteins and peptides from the four studies and removing replicates. This combined S-nitrosocysteine proteome consisted of 761 proteins and 1974 peptides (Fig. 2B).

3.3. S-nitrosylated protein abundance and occupancy

Analysis of the combined S-nitrosocysteine proteome in terms of relative protein expression revealed that most of the proteins are in the medium to high level of expression in the mouse heart (Fig. 3A). To perform this analysis, we constructed a mouse protein abundance database that consisted of 6301 proteins using data extracted from the integrated mouse heart proteome in the PAXdb: Protein Abundance Database. Moreover, the 80 proteins detected in all four studies are in the top quartile of relative abundance in the mouse heart (Fig. 3B). Collectively these observations suggest that protein abundance may be a factor for detecting S-nitrosylated proteins.

However, the percent occupancy, defined as the fraction of the peptide detected as S-nitrosylated over the sum of unmodified plus modified, did not appear to be a factor for the identification. We identified 75 S-nitrosocysteine residues in 44 proteins that were the same in all four studies. Occupancy in these common sites varied from 0.3 to 64% (Fig. 4A). A scatter plot of the average cysteine occupancy for proteins that had more than one peptide modified versus protein abundance did not reveal a significant correlation $R^2 = 0.039$, $N = 44$, data file 6). In the combined S-nitrosocysteine proteome, the occupancy for 1071 peptides varied from 0.1 to nearly 100%. Dividing these peptides into four quartiles revealed that a larger fraction, 803 S-nitrosocysteine peptides, had less than 26% occupancy whereas the occupancy of 144, 76 and 48 peptides were between 26 and 50%, 51–75% and 76–100% respectively (Fig. 4B). Together these observations suggest that occupancy is not a factor determining the detection of S-nitrosocysteine.

3.4. Functional analysis of the S-nitrosylated proteomes

The gene names of the proteins identified in each study were submitted to Gene Ontology and functional processes or cellular component (localization) were ranked based either on FDR value or fold enrichment. The analysis revealed an overwhelming functional clustering of the modified proteins in metabolic pathways and localization in mitochondria (Fig. 5 and data files 1–4). The top 20 functional categories in each independent study were metabolic pathways ranked either by the adjusted false discovery rate or percent enrichment (data files 1–4). The same was also observed when the entire combined S-nitrosocysteine

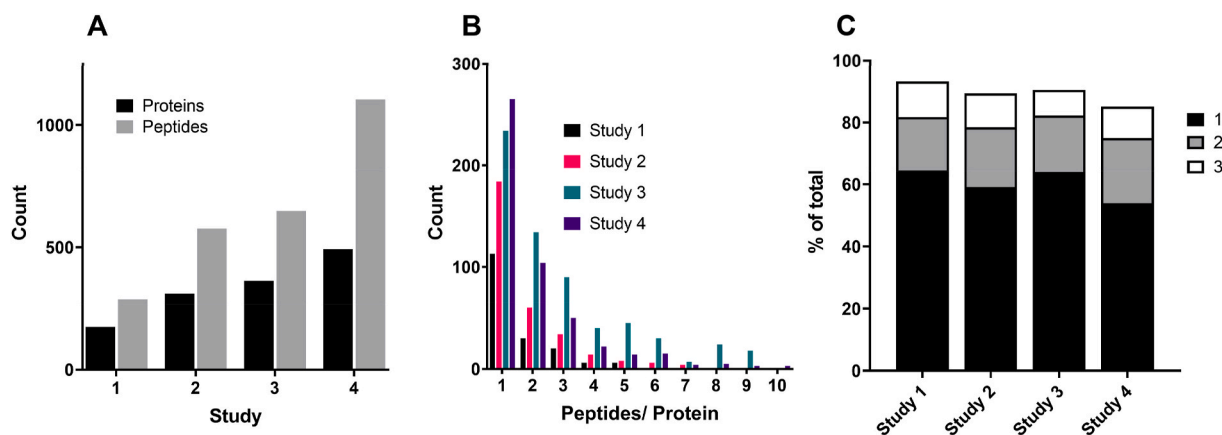


Fig. 1. A. Number of mouse heart proteins (canonical and isoforms) and peptides identified in the curated S-nitrosocysteine data sets for each independent study. B. The number of peptides per protein detected in each study. Not depicted in the graph are 3 proteins with 13 peptides identified in studies 3, and 7 proteins in study 4 with 11–26 peptides per protein respectively. C. The percentage of proteins with one, two or three cysteine residues modified in each study. The fraction of proteins with one, two or three modified cysteine residues was not statistically different among the four studies.

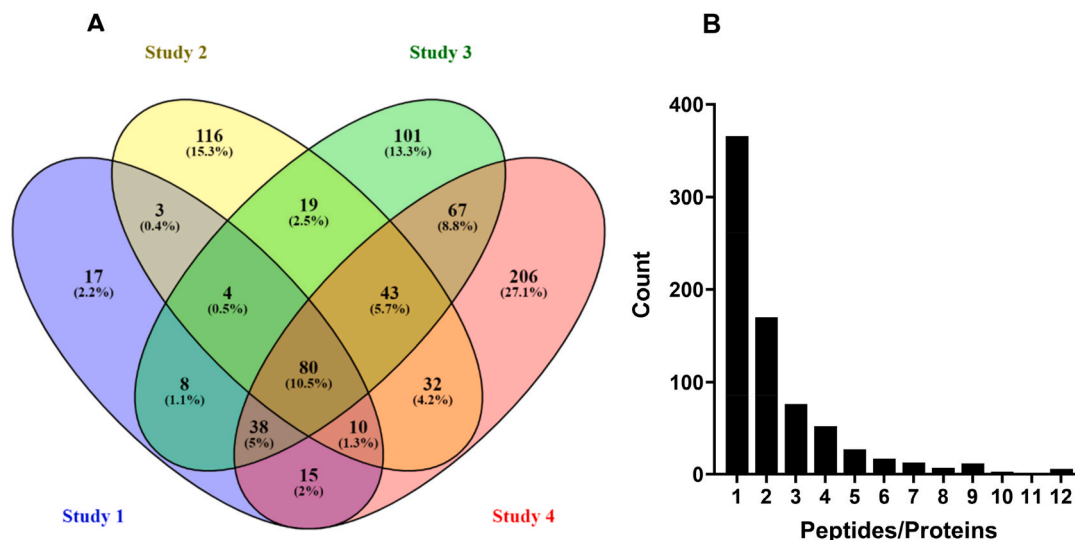


Fig. 2. A. Venn diagram depicting the overlap of the mouse heart proteins with S-nitrosocysteine residues in the four different studies. B. The distribution of peptides per protein of a combined S-nitrosocysteine proteome created by including all the unique proteins (both canonical and isoforms) and peptides identified in all four studies.

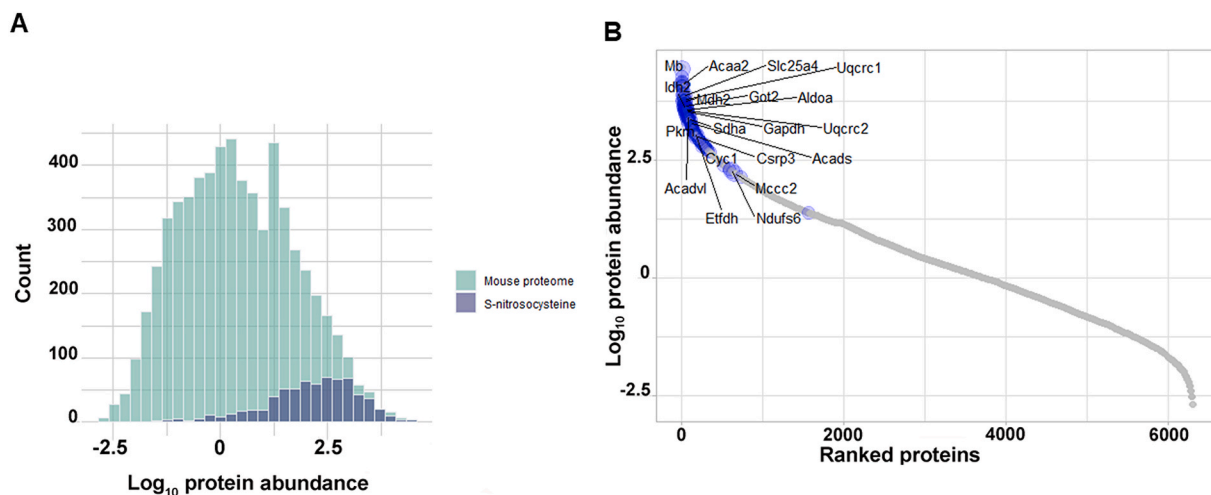


Fig. 3. A. Cumulative frequency of the relative abundance of 686 proteins in the combined S-nitrosocysteine proteome (blue) using the mouse heart protein abundance histogram as background (green). For the construction of the mouse heart protein abundance plot we curated data from the PAXdb: Protein Abundance Database using data from *Mus musculus* heart integrated from several independent mass spectrometric studies. B. The abundance of the 80 common proteins (blue dots) in the four studies among the 6301 mouse heart proteins (data file 6).

proteome was analyzed (data file 5). Moreover, 38 of the 44 proteins that shared the same modified cysteine residues are functionally annotated in cellular metabolism, glycolysis, generation of acetyl CoA from long chain fatty acid oxidation, the TCA cycle, amino acid and ketone metabolism, electron transport chain and ATP production/utilization (data file 6).

3.5. Biochemical attributes of the S-nitrosylated cysteine residues

We further analyzed key biochemical properties of the 75 S-nitrosocysteine residues in 44 proteins that were identified in all four studies (data file 7). As a comparison group we utilized 317 cysteine residues in the same 44 proteins that were not modified. The majority of the 317 cysteine residues were annotated as reduced. Cysteine residues 80, 85 in dihydrolipoyl dehydrogenase and 432, 439 in cardiac-type myosin-binding protein C formed disulfide bonds respectively. Consistent with previous data both the S-nitrosocysteine and unmodified cysteine residues exhibited roughly normal distribution with regards to the

hydropathy indices (Fig. 6A). The percent occupancy of the 75 S-nitrosylated cysteine residues did not correlate with the hydropathy index (Fig. 6B). Cysteine residues with relative high percent occupancy were localized within both hydrophilic and hydrophobic regions of the proteins. Utilizing data from available protein structures, we localized the secondary structure for 157 cysteine residues. Of the 157, 39 were S-nitrosocysteine and 118 unmodified residues. Unmodified cysteine residues within the same proteins were localized primarily in coils with lower frequency in helices and strands (Fig. 6C). This distribution is typical for cysteine residues in the proteome [18]. The modified S-nitrosocysteine residues reside primarily in strands and coils with only 4 localizing in helices (Fig. 6A). These data although limited in number are consistent with previous findings indicating the highest frequency of localization of S-nitrosocysteine residues in strands [16,18]. We investigated the apparent pKa value of the cysteine residues using available crystal structures and a web-based computational pKa prediction algorithm. The computed pKa of the S-nitrosylated cysteine residues was 9.49 ± 1.92 (N = 42) and 10.55 ± 2.31 (N = 117) for the unmodified

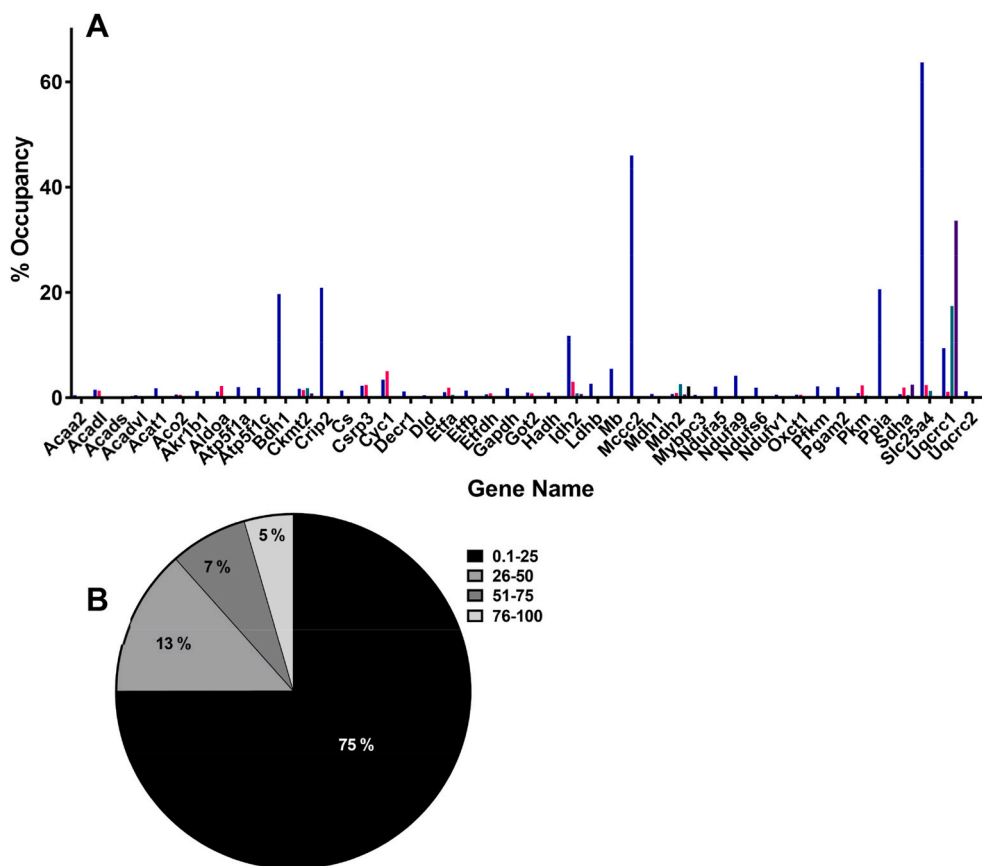


Fig. 4. A. The occupancy for each of the 75 peptides in the 44 proteins that were common in all four studies. Blue indicates the proteins with a single peptide. The other colors indicate different peptides in the same protein. B. The occupancy for 1071 peptides was divided into four quartiles. Most of the peptides (75%) had occupancy less than 26%.

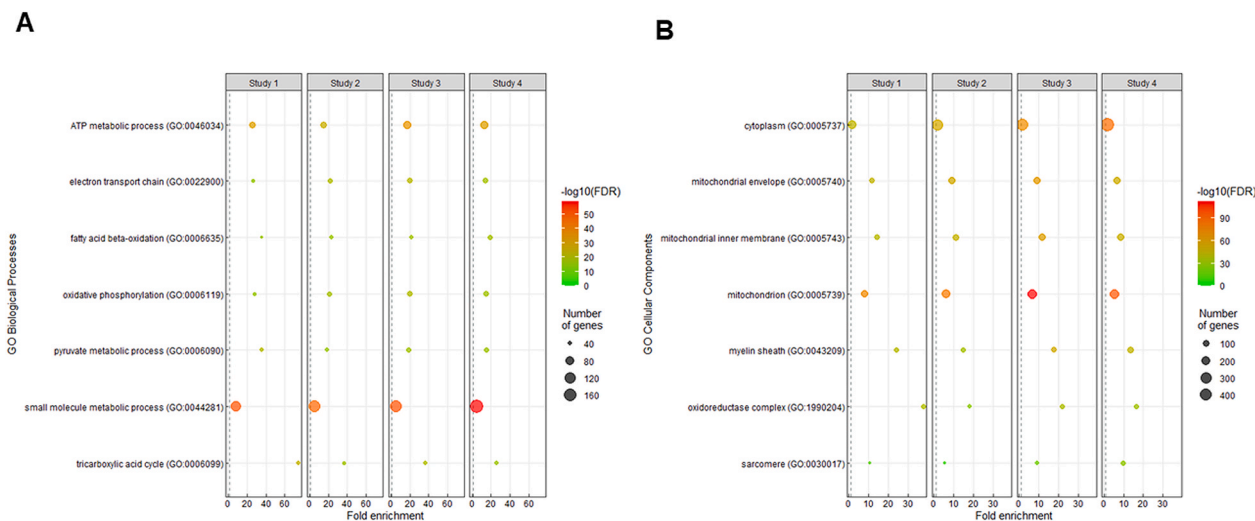


Fig. 5. Functional analysis of the proteins that are S-nitrosylated in each study. Panel A depicts selected biological processes and B the cellular component considering the values for FDR and fold enrichment. The size of the circle indicates the number of genes annotated in the corresponding biological process and cellular component. The selected biological processes and cellular components were in the top 20 annotations ranked by FDR in each study.

cysteine residues ($p < 0.01$). These data indicate that both modified and unmodified cysteine residues are protonated at physiological pH. However, we need to consider that these are average pKa values and that the local pKa can be affected by polar residues, which will cause a deviation between predicted and experimentally derived pKa.

Using data available from 21 S-nitrosocysteine peptides we

constructed a 3-dimensional plot using individual values for hydrophathy, pKa, and secondary structure (Fig. 7). Despite the limited number of data points the data indicates that basic biochemical properties do not predict the site or the magnitude of modification. Overall, consistent with previous data most of the biochemical properties of the modified cysteine residues are not unique as compared to unmodified cysteine

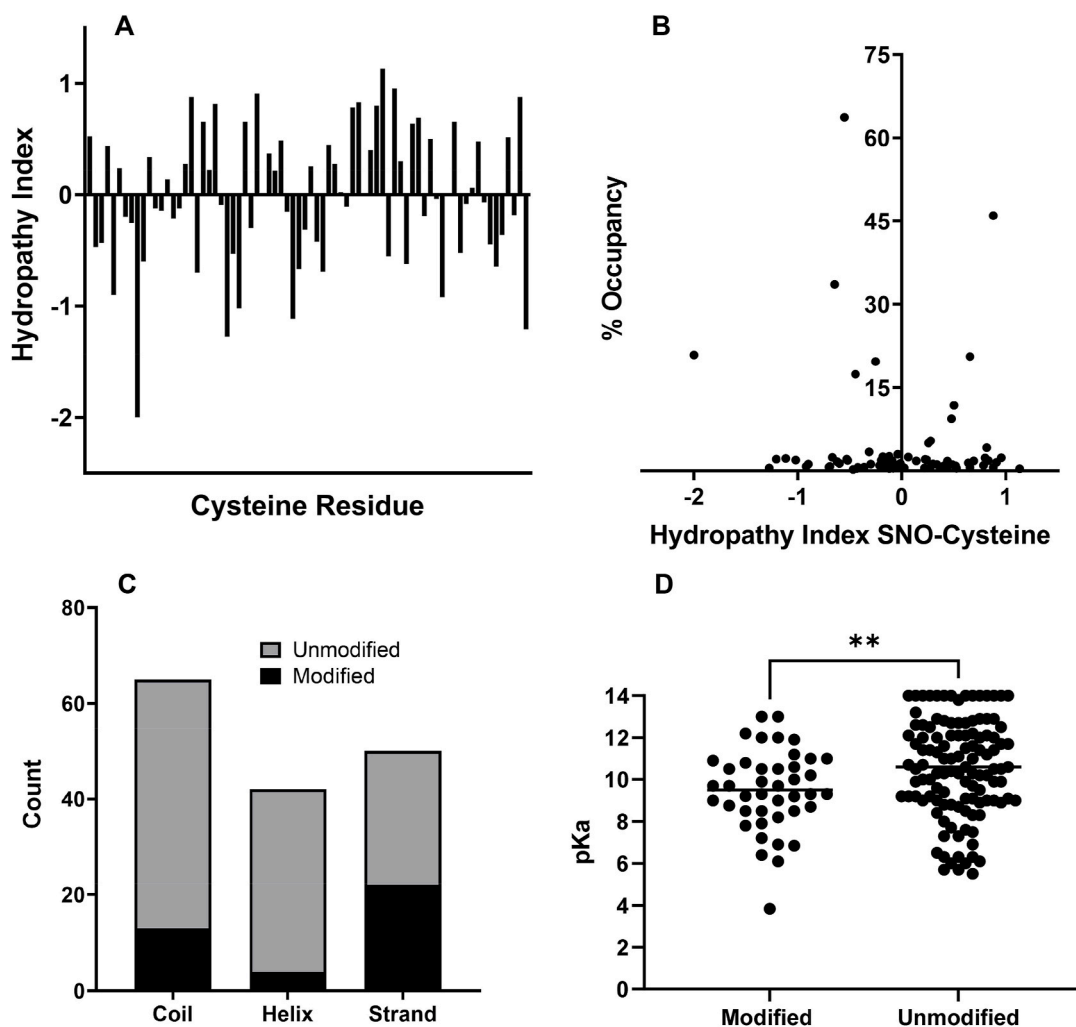


Fig. 6. A. Hydropathy index for each of the 75 S-nitrosylated cysteine residues indicating distribution in hydrophilic (negative value) and hydrophobic protein regions. B. The hydropathy index for each peptide was plotted against the percent occupancy indicating no correlation between the two variables. C. Distribution of S-nitrosocysteine residues (black) within secondary elements of proteins and the corresponding non-modified cysteine residues in the same proteins (grey). D. The apparent pKa of the S-nitrosylated cysteine residues was significantly ($N = 117$, $p < 0.01$) lower than of the unmodified cysteine residues.

residues and the basic biochemical properties of the cysteine residues did appear to dictate the yield of S-nitrosation [18].

4. Discussion

With the appropriate use of methodological platforms, controls and validation, proteins that are modified by nitric oxide *in vivo* have been revealed. This meta-analysis leveraged the existence of multiple proteomic studies in the same species (mouse) and organ (heart) that precisely identified endogenous S-nitrosocysteine residues in a physiological setting. By combining and curating the existing data [22–25] we generated a comprehensive list of 1974 S-nitrosocysteine residues in 761 proteins. The analysis revealed an overwhelming clustering of these proteins in basic metabolic pathways. This biological grouping was evident in the 761 proteins, the proteins identified in each independent study, as well as the 80 proteins that were identified in all four studies. These data suggest that protein S-nitrosylation in the mouse heart under physiological conditions fine tunes metabolic efficiency to secure uninterrupted production of ATP for the optimal contractile performance of the heart.

Before exploring the biological implications of this meta-analysis, we discuss the apparent reasons that may account for the disparities in the cysteine residues and proteins identified among the four studies. The

analysis indicated that 42.1% of the proteins were identified in two or more independent studies. Even fewer proteins, 10.5% were identified in all four studies and only 4% of the S-nitrosocysteine residues were the same across the 1974 cysteine residues identified. Several factors may contribute to these disparities and may arise from the methodology, biochemical and biophysical properties of S-nitrosocysteine residues and inherent biological variances. Steps in the methodological platforms that may account for the discordance in the data sets include the blocking of unmodified reduced cysteine residues, the generation and capture of nascent reduced cysteine residues, the procurement and processing of the biological samples, and the generation and detection of peptides by mass spectrometry. The well-known variability in the biochemical and biophysical properties of S-nitrosocysteine residues and of the reactivity of the nascent reduced cysteines generated after removal of NO towards different electrophiles may be additional contributors [16,18,40–43]. Differences in mouse age and tissue composition may represent biological variables. Although most of the data was collected from males, the age was not perfectly matched between the four studies. Study 4 used relative younger mice (2–2.5 months of age) whereas study 3 used mice up to 8 months old. Studies 1, 2 and 4 used the entire heart whereas study 3 used only left ventricles. Below we expand the discussion on the contributions of methodological issues and biochemical reactivity of cysteine residues to the variances in proteomic

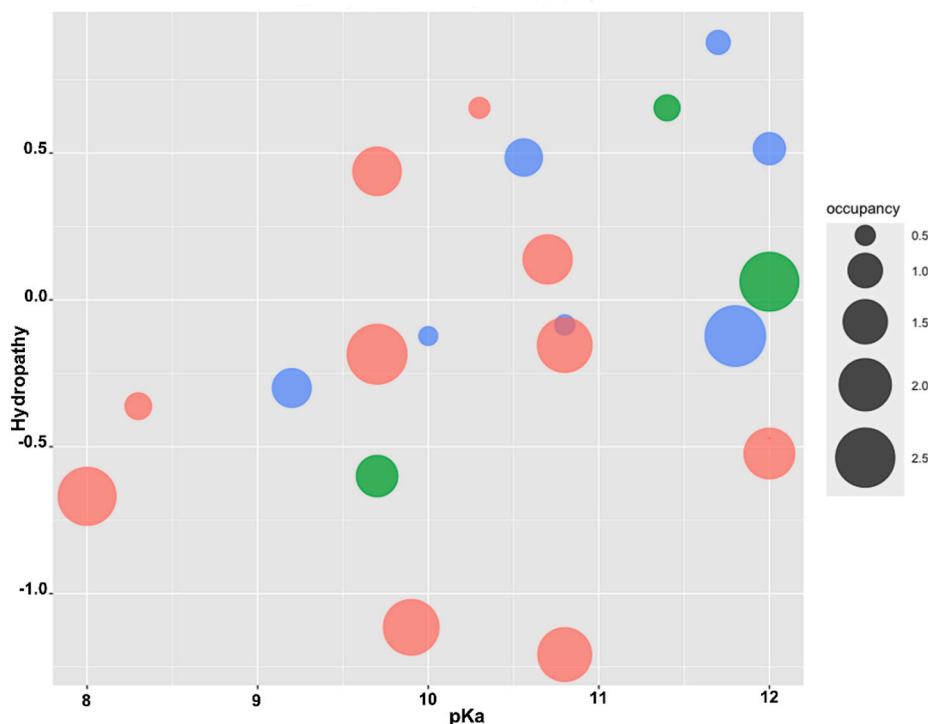


Fig. 7. Multidimensional plot of the biochemical properties and percent occupancy of S-nitrosylated cysteine residues. The pKa and hydropathy values are plotted in the x and y-axis respectively while the color of the bubble indicates the secondary element for each cysteine residue; Green indicates Helix, Red indicates Coil, and Blue indicates Strand. The size of the bubble is proportional to the percent S-nitrosylation for each residue. (For interpretation of the references to color in this figure legend, the reader is referred to the Web version of this article.)

detection.

The irreversible blocking of reduced cysteine residues with alkylating agents is a critical step to avoid false positive detection of peptides. Considering that the occupancy of S-nitrosylation is sub-stoichiometric, even 99% blocking efficiency would lead to misidentifications of cysteine residues. For example, since the average levels of reduced cysteine are in the order of 10 μ M, the concentration of the 1% of unblocked residues will be 100 nM, which is about the same as total protein S-nitrosocysteine levels [16]. Previously, we have indicated that negative controls for each sample analyzed are crucial to remove potential false positive identifications and we recommend routine use of negative controls in all proteomic experiments [16].

Another step that contributes to the variances is the reduction of the S-nitrosocysteine residues to generate reduced cysteine and the recapture of the reduced cysteine with various tags. During the reduction step with ascorbate or ascorbate plus copper, there is a potential reduction of disulfides, other protein mix-disulfides such as S-gluthionylated or S-sulfhydrylated cysteine residues and even oxidized sulfenic acid that could generate false positive detection. Another contributing factor in the switch-based approaches may relate to the reactivity of the newly reduced cysteine residues towards different tags used to recapture and label these residues. A carefully conducted and highly informative study performed by Chug et al. [24] explored the use of two different tags, cysteine-reactive tandem mass tag and iodoacetyl tandem mass tag on the same biological sample. The data reported that approximately 32% of the peptides identified by each tag were shared. Considering these challenges, we have implemented a direct approach to displace NO and capture the reduced cysteine residues by exploiting the well-known Saville chemistry between S-nitrosocysteine with organic mercury [16]. Although our approach avoids the two-step process, it has a similar depth of identification as the other studies but also shows similar discordance as the two-step methods. Therefore, the reactivity of the S-nitrosylated and reduced cysteine towards different molecules may be a significant contributor for the variances.

This issue is not unique to the identification of S-nitrosocysteine residues. Proteomic studies that identify endogenously phosphorylated peptides have similar discordance based on the chemical platforms used

for the enrichment step. For example, identical samples were enriched for phosphopeptides using the two most common enrichment platforms, the immobilized metal affinity chromatography (IMAC) and metal oxide affinity chromatography with TiO₂ [44]. Three rounds of IMAC enrichment resulted in the identification of 5272 phosphopeptides whereas three rounds of TiO₂ enrichment identified 4918 phosphopeptides. Only 34% of the phosphopeptides were identified by both IMAC and TiO₂ enrichment. Several biochemical and biophysical parameters including single monophosphorylated vs multisite peptides, the length of peptide, pI value, hydrophobicity of phosphopeptides (GRAVY values), motifs (surrounding residues in linear sequence) contributed to the differences in detection between the IMAC and TiO₂ enrichment platforms [44].

The formation of more reactive deprotonated thiolate cysteine residues has been considered a primary feature of cysteine reactivity. Other studies indicated that thiolate formation is only one factor that governs reactivity and additional parameters such as hydropathy, and solvent accessibility, pKa values and charged amino acid frequency in the vicinity of the cysteine residue may contribute to the chemical reactivity [16,18,40–42]. However, the remarkable reactivity of certain cysteine residues is mostly independent of the biophysical properties but is fine-tuned to specific post-translational modifications, including S-nitrosylation [18]. These observations indicate that the use of a single methodological platform to identify the S-nitrosoproteome although informative, may be inefficient. Future experiments should consider the use of multiple approaches combined with negative controls to improve the precision and depth of analysis.

Another often overlooked contribution comes from the process of peptide generation and detection by mass spectrometry. Variations in protein extraction from the heart tissue could lead to differences in proteins and peptides identified. Although the methods for efficient and reproducible trypsin or other enzymatic digestion to generate peptides for mass spectrometric detection have been streamlined, small variations could influence the outcome. Similarly, detection of peptides by mass spectrometry is a stochastic process, indicating that enough replicates are needed to secure reproducible detection of a given peptide. Improvements in mass spectrometry platforms have improved peptide

detection making this step a minor contributor to the variances observed.

Finally, sample collection and processing that influence protein extraction and the ex-vivo stability of protein S-nitrosocysteine must be considered. The relative enrichment for metabolic proteins, most localized in mitochondria, may result from the high mitochondria content in heart tissue. Alternatively, it may result from tissue homogenization and protein extraction methodologies that may favor mitochondrial protein enrichment over more difficult to extract structural proteins participating in cardiomyocyte contraction. For example, studies 1 and 3 utilized homogenization methods that favor mitochondrial protein extraction and preservation, studies 2 and 4 did not. The relative enrichment for mitochondrial proteins was 8.06, 6.30, 6.64 and 5.41 whereas the enrichment for contractile fiber was 8.82, 5.49, 7.74, and 9.44 for studies 1–4 respectively. Therefore, the enrichment for metabolic proteins may be routed in the relative high abundance of these proteins in the heart or the biological selectivity of S-nitrosylation targeting metabolic pathways.

The importance of executing sample collection and processing samples as rapidly as possible in the dark to minimize light-induced decomposition of S-nitrosocysteine was considered in all studies. Using mild alkaline buffers and inclusion of metal chelators including the copper chelator neocuproine are essential to preserve the S-nitrosocysteine residues. It is therefore possible that most of the S-nitrosocysteine residues identified represent the more stable sites as suggested previously [45]. However, it does not indicate biologically stable or long-lasting S-nitrosocysteine residues, but rather ex vivo stability. Since the proteomes in all four studies are static snapshots, conclusions about biological stability and half-life cannot be made. While relative protein abundance may be a factor in the detection of the proteins, the occupancy (fraction of S-nitrosocysteine as compared to same unmodified cysteine residue) is not. Clearly, there is need for additional studies exploring the half-life of modified proteins *in vivo* to appreciate the stability of the modification and the influence of the modification on the dynamic turnover of modified proteins. By now several chemical and enzymatic pathways have been identified for both the formation and removal of protein S-nitrosocysteine residues predicting an expected biological variability like many other post-translational modifications. Additional structural analysis to correlate conformational stability and reactivity of S-nitrosocysteine residues with protein turnover and functionality will be highly informative.

The biological functions of nitric oxide signaling in the heart and cardiovascular system have been firmly established in both humans and animal models [46–53]. The utilization of mice deficient in one, to all three major NOS isoforms indicated that in addition to vasorelaxation, NO signaling regulates cardiac contractility and responses of cardiomyocytes to inotropic and lusitropic agents [46,50]. The analyses of the *in vivo* S-nitrosocysteine proteome offer an additional regulatory function of NO signaling—the regulation of metabolic efficiency. Cardiac muscle contractile performance relies on hemodynamics and metabolism. Adequate blood flow is needed to deliver oxygen and metabolites for the efficient generation of ATP. It is estimated that greater than 95% of the cardiac ATP production is derived from oxidative phosphorylation and approximately 60–70% of the ATP generated is used to support the continuous mechanical work of the cardiomyocytes. To meet this constant demand for ATP, the cardiomyocytes rely on having an adequate number of effectively working mitochondria. They also rely on an adequate supply of fatty acids and fatty acid β -oxidation which generates nearly 70% of acetyl-CoA utilized for ATP production. The remaining ATP is generated from the oxidation of glucose and lactate, as well as small amounts of ketone bodies and amino acids [54,55]. Therefore, signaling pathways that coordinate metabolism and secure adequate production of ATP are also critical contributors to the performance of the heart. The functional analyses of the proteomic data indicated that protein S-nitrosylation may represent one of the signaling pathways that optimizes metabolic efficiency. This suggestion is in part

supported by data in other organs where protein S-nitrosylation was shown to regulate metabolism. For example, S-nitrosylation of proteins participating in β -oxidation in the mouse liver promotes acetyl-CoA generation from long chain fatty acid oxidation [23]. S-nitrosylation of pyruvate kinase M2 which regulates the last step in glycolysis (conversion of phosphoenolpyruvate to pyruvate) was shown to protect the kidney from ischemia/reperfusion injury [19]. Mechanistically the protection was attributed to the reprogramming in metabolism, shifting glucose oxidation to the pentose phosphate shunt to augment reductive and antioxidant capacity.

Based on experimental evidence others and we have suggested that protein S-nitrosylation targets multiple proteins clustered within specific biological pathways [10,11,18]. This implies a coordinated action to regulate the entire pathway and secure that the signal is transmitted in a timely manner to maximize pathway performance. Metabolic pathways are prime examples since spatiotemporal regulation through the coordinated action of nitrosylases and denitrosylases has been reported [14,15,17,19,20]. We posit that dynamic changes of S-nitrosylation occupancy are part of this coordinated response ensuring adequate flow of intermediates across different metabolic pathways to avoid metabolic gridlocks. Examples include the coordination of long chain fatty acid oxidation and glycolysis to secure adequate flow of acetyl CoA to the TCA cycle, the utilization of anaplerotic substrates for the TCA cycle and the production and utilization of ketones. For the heart, NO signaling via the canonical guanylate cyclase-cGMP pathway and protein S-nitrosylation contributes to coronary epicardial and microvascular relaxation to provide adequate delivery of oxygen and metabolites, facilitate cardiac contractility, and optimize metabolic efficiency to ensure optimal heart performance.

5. Availability of data and material

All data analyzed during this study are included in this published article and its Supplementary files.

Authors' contributions

BL collected, wrote scripts and analyzed data, HF generated data and Figs. 3, 5 and 7, IM and SR analyzed data and performed quality checks on the final curated proteomes, MT and PTD analyzed peptide data and contributed Fig. 6. HI planned, organized, and participated in the analysis and discussion of all the data, writing and editing of the manuscript. All authors contributed in writing, editing and approving the final manuscript.

Funding

These studies were supported by the Gisela and Dennis Alter Endowed Chair in Pediatric Neonatology (HI).

Declaration of competing interest

The authors declare no competing interests.

Acknowledgements

The authors thank Drs. Ding Hua and Lynn Spruce at the Proteomics Core Facility at the Children's Hospital of Philadelphia Research Institute, for their support and discussions regarding the proteomic analyses.

Appendix. BSupplementary data

Supplementary data to this article can be found online at <https://doi.org/10.1016/j.redox.2021.102153>.

Appendix A. Supplementary data

Supplementary data file 1: Study 1 original and curated proteomic data.

Supplementary data file 2: Study 2 original and curated proteomic data.

Supplementary data file 3: Study 3 original and curated proteomic data.

Supplementary data file 4: Study 4 original and curated proteomic data.

Supplementary data file 5: Study 1–4 combined proteomic data.

Supplementary data file 6: Analysis of common proteins.

Supplementary data file 7: Peptide analysis.

References

- [1] R.F. Furchgott, The 1996 Albert Lasker Medical Research Awards. The discovery of endothelium-derived relaxing factor and its importance in the identification of nitric oxide, *J. Am. Med. Assoc.* 276 (1996) 1186–1188.
- [2] F. Murad, Shattuck Lecture. Nitric oxide and cyclic GMP in cell signaling and drug development, *N. Engl. J. Med.* 355 (2006) 2003–2011.
- [3] L.J. Ignarro, Nitric oxide: a unique endogenous signaling molecule in vascular biology, *Biosci. Rep.* 19 (1999) 51–71.
- [4] S. Moncada, E.A. Higgs, The discovery of nitric oxide and its role in vascular biology, *Br. J. Pharmacol.* 147 (2006) S193–S201.
- [5] T.M. Lincoln, X. Wu, H. Sellak, N. Dey, C.S. Choi, Regulation of vascular smooth muscle cell phenotype by cyclic GMP and cyclic GMP-dependent protein kinase, *Front. Biosci.* 11 (2006) 356–367.
- [6] E.J. Tsai, D.A. Kass, Cyclic GMP signaling in cardiovascular pathophysiology and therapeutics, *Pharmacol. Ther.* 122 (2009) 216–238.
- [7] S.H. Francis, The role of cGMP-dependent protein kinase in controlling cardiomyocyte cGMP, *Circ. Res.* 107 (2010) 1164–1166.
- [8] S.H. Francis, M.A. Blount, J.D. Corbin, Mammalian cyclic nucleotide phosphodiesterases: molecular mechanisms and physiological functions, *Physiol. Rev.* 91 (2011) 651–690.
- [9] J.S. Stamler, D.I. Simon, J.A. Osborne, M.E. Mullins, O. Jaraki, T. Michel, D. J. Singel, J. Loscalzo, S-nitrosylation of proteins with nitric oxide: synthesis and characterization of biologically active compounds, *Proc. Natl. Acad. Sci. U. S. A.* 89 (1992) 444–448.
- [10] D. Seth, J.S. Stamler, The SNO-proteome: causation and classifications, *Curr. Opin. Chem. Biol.* 15 (2011) 129–136.
- [11] B.C. Smith, M.A. Marletta, Mechanisms of S-nitrosothiol formation and selectivity in nitric oxide signaling, *Curr. Opin. Chem. Biol.* 16 (2012) 498–506.
- [12] N. Gould, P.T. Doulias, M. Tenopoulou, K. Raju, H. Ischiropoulos, Regulation of protein function and signaling by reversible cysteine S-nitrosylation, *J. Biol. Chem.* 288 (2013) 26473–26479.
- [13] L. Liu, Y. Yan, M. Zeng, J. Zhang, M.A. Hanes, G. Ahearn, T.J. McMahon, T. Dickfeld, H.E. Marshall, L.G. Que, J.S. Stamler, Essential roles of S-nitrosothiols in vascular homeostasis and endothotic shock, *Cell* 116 (2004) 617–628.
- [14] D.A. Mitchell, M.A. Marletta, Thioredoxin catalyzes the S-nitrosation of the caspase-3 active site cysteine, *Nat. Chem. Biol.* 1 (2005) 154–158.
- [15] K.T. Barglow, C.G. Knutson, J.S. Wishnok, S.R. Tannenbaum, M.A. Marletta, Site-specific and redox-controlled S-nitrosation of thioredoxin, *Proc. Natl. Acad. Sci. U. S. A.* 108 (2011) E600–E606.
- [16] T.-P. Doulias, J.K. Greene, T.M. Greco, M. Tenopoulou, S.H. Seeholzer, R. L. Dunbrack, H. Ischiropoulos, Structural profiling of endogenous S-nitrosocysteine residues reveals unique features that accommodate diverse mechanisms for protein S-nitrosylation, *Proc. Natl. Acad. Sci. U. S. A.* 107 (2010) 16958–16963.
- [17] J. Jia, A. Arif, F. Terenzi, B. Willard, E.F. Plow, S.L. Hazen, P.L. Fox, Target-selective protein S-nitrosylation by sequence motif recognition, *Cell* 159 (2014) 623–634.
- [18] N.S. Gould, P. Evans, P. Martínez-Acedo, S.M. Marino, V.N. Gladyshev, K. S. Carroll, H. Ischiropoulos, Site-specific proteomic mapping identifies selectively modified regulatory cysteine residues in functionally distinct protein networks, *Chem. Biol.* 22 (2015) 965–975.
- [19] H.L. Zhou, R. Zhang, P. Anand, C.T. Stomberski, Z. Qian, A. Hausladen, L. Wang, E. P. Rhee, S.M. Parikh, S.A. Karumanchi, J.S. Stamler, Metabolic reprogramming by the S-nitroso-CoA reductase system protects against kidney injury, *Nature* 565 (2019) 96–100. Erratum in: *Nature*. 2019;570:E23.
- [20] M. Benhar, M.T. Forrester, D.T. Hess, J.S. Stamler, Regulated protein denitrosylation by cytosolic and mitochondrial thioredoxins, *Science* 320 (2008) 1050–1054.
- [21] S.R. Jaffrey, H. Erdjument-Bromage, C.D. Ferris, P. Tempst, S.H. Snyder, Protein S-nitrosylation: a physiological signal for neuronal nitric oxide, *Nat. Cell Biol.* 3 (2001) 193.
- [22] M.J. Kohr, A. Aponte, J. Sun, M. Gucek, C. Steenbergen, E. Murphy, Measurement of S-nitrosylation occupancy in the myocardium with cysteine-reactive tandem mass tags: short communication, *Circ. Res.* 111 (2012) 1308–1312.
- [23] P.-T. Doulias, M. Tenopoulou, J.L. Greene, K. Raju, H. Ischiropoulos, Nitric oxide regulates mitochondrial fatty acid metabolism through reversible protein S-nitrosylation, *Sci. Signal.* 6 (2013) rs1–7. PMID: 23281369, PMCID: PMC4010156.
- [24] H.S. Chung, C.I. Murray, V. Venkatraman, E.L. Crowgey, P.P. Rainer, R.N. Cole, R. D. Bomgardner, J.C. Rogers, W. Balkan, J.M. Hare, D.A. Kass, J.E. Van Eyk, Dual labeling biotin switch assay to reduce bias derived from different cysteine subpopulations: a method to maximize S-nitrosylation detection, *Circ. Res.* 117 (2015) 846–857.
- [25] E.T. Chouchani, A.M. James, C. Methner, V.R. Pell, T.A. Prime, B.K. Erickson, M. Forkink, G.Y. Lau, T.P. Bright, K.E. Menger, I.M. Fearley, T. Krieg, M. P. Murphy, Identification and quantification of protein S-nitrosation by nitrite in the mouse heart during ischemia, *J. Biol. Chem.* 292 (2017) 14486–14495.
- [26] D. Su, A.K. Shukla, B. Chen, J.S. Kim, E. Nakayasu, Y. Qu, U. Aryal, K. Weitz, T. R. Clauss, M.E. Monroe, D.G. Camp 2nd, D.J. Bigelow, R.D. Smith, R.N. Kulkarni, W.J. Qian, Quantitative site-specific reactivity profiling of S-nitrosylation in mouse skeletal muscle using cysteinyl peptide enrichment coupled with mass spectrometry, *Free Radic. Biol. Med.* 57 (2013) 68–78.
- [27] C.I. Murray, H. Uhrigshardt, R.N. O’Meally, R.N. Cole, J.E. Van Eyk, Identification and quantification of S-nitrosylation by cysteine reactive tandem mass tag switch assay, *Mol. Cell. Proteomics* 11 (2012), 013441. M111.
- [28] H.S. Chung, G.E. Kim, R.J. Holeywinski, V. Venkatraman, G. Zhu, D. Bedja, D. A. Kass, J.E. Van Eyk, Transient receptor channel 6 regulates abnormal cardiac S-nitrosylation in Duchenne muscular dystrophy, *Proc. Natl. Acad. Sci. U. S. A.* 114 (2017) E10763–E10771.
- [29] K. Raju, P.T. Doulias, P. Evans, E.N. Krizman, J.G. Jackson, O. Horyn, Y. Daikhin, I. Nissim, M. Yudkoff, I. Nissim, K.A. Sharp, M.B. Robinson, H. Ischiropoulos, Regulation of brain glutamate metabolism by nitric oxide and S-nitrosylation, *Sci. Signal.* 8 (2015) ra68.
- [30] M. Zareba-Kozioł, A. Bartkowiak-Kaczmarek, I. Figiel, A. Krzysztyniak, T. Wojtowicz, M. Bijata, J. Włodarczyk, Stress-induced changes in the S-palmitoylation and S-nitrosylation of synaptic proteins, *Mol. Cell. Proteomics* 18 (2019) 1916–1938.
- [31] Uthpala Seneviratne, Alexi Nott, Vadiraja B. Bhat, Kodihalli C. Ravindra, John S. Wishnok, Li-Huei Tsai, Steven R. Tannenbaum, S-nitrosation of proteins relevant to Alzheimer’s disease during early stages of neurodegeneration, *Proc. Natl. Acad. Sci. U. S. A.* 113 (2016) 4152–4157.
- [32] H. Amal, G. Gong, E. Gjonneska, et al., S-nitrosylation of E3 ubiquitin-protein ligase RNF213 alters non-canonical Wnt/Ca²⁺ signaling in the P301S mouse model of tauopathy, *Transl. Psychiatry* 9 (2019) 44.
- [33] Y. Zhou, S.L. Wynia-Smith, S.M. Couvartier, K.S. Kalous, M.A. Marletta, B.C. Smith, E. Weerapana, Chemoproteomic strategy to quantitatively monitor transnitrosation uncovers functionally relevant S-nitrosation sites on cathepsin D and HADH2, *Cell Chem Biol* 23 (2016) 727–737.
- [34] R. Mnatsakanyan, S. Markoutsas, K. Walbrunn, A. Roos, S.H.L. Verhelst, R. P. Zahedi, Proteome-wide detection of S-nitrosylation targets and motifs using biorthogonal cleavable-linker-based enrichment and switch technique, *Nat. Commun.* 10 (2019) 2195.
- [35] The UniProt Consortium, UniProt: the universal protein knowledgebase in 2021, *Nucleic Acids Res.* 49 (Issue D1) (8 January 2021) D480–D489.
- [36] M. Wang, C.J. Herrmann, M. Simonovic, D. Szklarczyk, C. von Mering, Version 4.0 of PaxDb: protein abundance data, integrated across model organisms, tissues, and cell-lines, *Proteomics* 15 (18) (2015 Sep) 3163–3168.
- [37] Ashburner, et al., Gene ontology: tool for the unification of biology, *Nat. Genet.* 25 (1) (May 2000) 25–29.
- [38] The Gene Ontology resource: enriching a GOLD mine, *Nucleic Acids Res.* 49 (D1) (Jan 2021) D325–D334.
- [39] Hui Li, Andrew D. Robertson, Jan H. Jensen, Very fast empirical prediction and interpretation of protein pKa values, *Proteins* 61 (2005) 704–721.
- [40] D. Seth, J.S. Stamler, SNOs Differ: methodological and biological implications, *Circ. Res.* 117 (2015) 826–829.
- [41] S.M. Marino, V.N. Gladyshev, Cysteine function governs its conservation and degradation and restricts its utilization on protein surfaces, *J. Mol. Biol.* 404 (2010) 902–916.
- [42] E. Weerapana, C. Wang, G.M. Simon, F. Richter, S. Khare, M.B. Dillon, D. A. Bachovchin, K. Mowen, D. Baker, B.F. Cravatt, Quantitative reactivity profiling predicts functional cysteines in proteomes, *Nature* 468 (2010) 790–795.
- [43] Y. Shi, K.S. Carroll, Activity-based sensing for site-specific proteomic analysis of cysteine oxidation, *Acc. Chem. Res.* 53 (2020) 20–31.
- [44] G.T. Cantin, T.R. Shock, S.K. Park, H.D. Madhani, J.R. Yates 3rd, Optimizing TiO₂-based phosphopeptide enrichment for automated multidimensional liquid chromatography coupled to tandem mass spectrometry, *Anal. Chem.* 79 (2007) 4666–4673.
- [45] K. Wolhuter, H.J. Whitwell, C.H. Switzer, J.R. Burgoyne, J.F. Timms, P. Eaton, Evidence against stable protein S-nitrosylation as a widespread mechanism of post-translational regulation, *Mol. Cell.* 69 (2018) 438–450, e5.
- [46] P.L. Huang, eNOS, metabolic syndrome and cardiovascular disease, *Trends Endocrinol. Metabol.* 20 (2009) 295–302.
- [47] L.A. Barouch, R.W. Harrison, M.W. Skaf, G.O. Rosas, T.P. Cappola, Z.A. Kobeissi, et al., Nitric oxide regulates the heart by spatial confinement of nitric oxide synthase isoforms, *Nature* 416 (2002) 337–339.
- [48] A.A. Quyyumi, N. Dakak, N.P. Andrews, D.M. Gilligan, J.A. Panza, R. O. Cannon 3rd, Contribution of nitric oxide to metabolic coronary vasodilation in the human heart, *Circulation* 92 (3) (1995 Aug 1) 320–326, <https://doi.org/10.1161/01.cir.92.3.320>. PMID: 7634444.
- [49] J. Erdmann, K. Stark, U.B. Esslinger, P.M. Rumpf, D. Koesling, et al., Dysfunctional nitric oxide signalling increases risk of myocardial infarction, *Nature* 504 (2013) 432–436.

- [50] M. Tsutsui, A. Tanimoto, M. Tamura, H. Mukae, N. Yanagihara, H. Shimokawa, et al., Significance of nitric oxide synthases: lessons from triple nitric oxide synthases null mice, *J. Pharmacol. Sci.* 127 (1) (2015) 42–52.
- [51] J.O. Lundberg, M.T. Gladwin, E. Weitzberg, Strategies to increase nitric oxide signalling in cardiovascular disease, *Nat. Rev. Drug Discov.* 4 (2015) 623–641.
- [52] T. Irie, P.Y. Sips, S. Kai, K. Kida, K. Ikeda, S. Hirai, K. Moazzami, P. Jiramongkolchai, D.B. Bloch, P.T. Doulias, A.A. Armoundas, M. Kaneki, H. Ischiropoulos, E. Kranias, K.D. Bloch, J.S. Stamler, F. Ichinose, S-nitrosylation of calcium-handling proteins in cardiac adrenergic signaling and hypertrophy, *Circ. Res.* 117 (2015) 793–803.
- [53] E.T. Chouchani, C. Methner, S.M. Nadtochiy, A. Logan, V.R. Pell, S. Ding, A. M. James, H.M. Cochemé, J. Reinhold, K.S. Lilley, L. Partridge, I.M. Fearnley, A. J. Robinson, R.C. Hartle, R.A. Smith, T. Krieg, P.S. Brookes, M.P. Murphy, Cardioprotection by S-nitrosation of a cysteine switch on mitochondrial complex I, *Nat. Med.* 19 (2013) 753–759.
- [54] H. Taegtmeyer, M.E. Young, G.D. Lopaschuk, Abel, et al., Assessing cardiac metabolism A scientific statement from the American heart association, *Circ. Res.* 118 (2016) 1659–1701.
- [55] G.D. Lopaschuk, J.R. Ussher, C.D. Folmes, J.S. Jaswal, W.C. Stanley, Myocardial fatty acid metabolism in health and disease, *Physiol. Rev.* 90 (2010) 207–258.